NRC Publications Archive
Archives des publications du CNRC

Natural gas spark ignition engine efficiency and NOx emission improvement using extreme exhaust gas recirculation enabled by partial reforming
Hosseini, V.; Checkel, M. D.; Neill, W. S.

National Research Council Canada   Conseil national de recherches Canada

Canada

Natural gas spark ignition engine efficiency and NO_x emission improvement using extreme exhaust gas recirculation enabled by partial reforming

V Hosseini[1]*, M D Checkel[2], and W S Neill[1]

[1]Institute for Chemical Process and Environmental Technology, Canada National Research Council, Ottawa, Ontario, Canada

[2]Mechanical Engineering Department, University of Alberta, Edmonton, Alberta, Canada

Abstract: Natural-gas (NG), spark ignition (SI) engines have widespread application in the power generation and upstream oil and gas industries. The manufacturers of these engines are being challenged to meet increasingly stringent nitrogen oxide (NO_x) emission regulations without sacrificing fuel conversion efficiency.

SI engines may be operated with air–fuel mixtures lean of stoichiometric to achieve higher thermal efficiency and to reduce NO_x emissions. Compared with new combustion strategies such as homogeneous charge compression ignition, however, lean SI combustion suffers from a somewhat limited tolerability to mixture dilution and high cyclic variations. Alternatively, NO_x emissions may be reduced by using exhaust gas recirculation (EGR) to dilute a stoichiometric air–fuel mixture. This paper investigates the application of reformer gas (RG) to enable a higher mixture dilution of an NG SI engine using EGR.

It was found that RG enrichment allows an increase in the EGR dilution of a stoichiometric NG–air mixture from 12 per cent to more than 35 per cent. The optimal level of RG enrichment directly compensates for the combustion phasing retardation effect of EGR. Increasing the RG fraction in the mixture beyond the optimal value adversely affected the combustion process and fuel conversion efficiency. The experimental data suggest that NO_x emissions comparable with the forthcoming 2010 US Environmental Protection Agency heavy-duty diesel engine regulations may be achieved using EGR, RG enrichment, and a three-way catalytic converter (TWC).

An energy balance showed that there is the potential to increase the overall system fuel conversion efficiency slightly owing to a more optimized combustion process after taking into account the energy losses associated with fuel reforming. The approach of EGR, fuel reforming, and a TWC is suitable for retrofits because it can be accomplished without modifying the engine geometry.

Keywords: efficiency, natural-gas spark ignition engine, nitrogen oxide emission, extreme exhaust gas recirculation, partial reforming

1 INTRODUCTION

Reducing nitrogen oxide (NO_x) emissions presents a major challenge of internal combustion engine designers as increasingly stringent emission standards come into effect. For example, the US Environmental Protection Agency (EPA) has phased in new NO_x emission standards of 0.20 g/bhp h (0.27 g/kW h) for heavy-duty highway engines, beginning in model year 2007 [1].

Several emission control technologies have been implemented for spark ignition (SI) and compression ignition engines to reduce NO_x emissions from

Corresponding author: Institute for Chemical Process and Environmental Technology, Canada National Research Council, M-9, 1200 Montreal Road, Ottawa, Ontario, K1A 0R6, Canada. email: vahid.hosseini@nrc-cnrc.gc.ca

JAUTO539 © IMechE 2008

Proc. IMechE Vol. 222 Part D: J. Automobile Engineering

the exhaust stream. Three-way catalytic converter (TWC) technology is widely used to reduce NO_x, unburned hydrocarbon (HC), and carbon monoxide (CO) emissions simultaneously from SI engines in the automotive sector. Lean NO_x traps and selective catalytic reduction are two emission control technologies used for non-stoichiometric mixtures. Since emission control technologies add cost and complexity to a power plant, minimizing NO_x formation during the combustion process by reducing the peak combustion chamber temperatures is generally the preferred solution.

High-efficiency clean combustion (HECC) is the name given to advanced low-temperature combustion strategies being developed to reduce NO_x formation inside the combustion chamber while maintaining or increasing the fuel conversion efficiency level of current engines. The peak temperatures during the combustion process are typically reduced by diluting the air–fuel mixture with excess air and/ or recirculated exhaust gases. For liquid fuels, this can be achieved using either a homogeneous-charge or mixing-controlled strategy.

For stationary industrial engines operated with natural gas (NG), the autoignition properties of NG make both homogeneous-charge and mixing-controlled HECC strategies problematic. This paper proposes to address this difficulty in NG-fuelled SI engines by operating the engines with a stoichiometric air-to-fuel ratio and extending the exhaust gas recirculation (EGR) dilution limit using reformer gas (RG). A TWC can still be used under these conditions to reduce NO_x emissions further.

1.1 Reformer gas

RG is a mixture of light gases dominated by hydrogen (H_2), CO, carbon dioxide (CO_2), nitrogen (N_2), and water (H_2O) that can be produced from NG and other HCs by partial oxidation or steam reforming.

Table 1 compares a number of the combustion-related properties of the two main components of RG, H_2, and CO with those of NG and gasoline.

Fuel reforming can be achieved by partial oxidation, steam reforming, or autothermal reforming (which combines partial oxidation, steam reforming, and the water–gas shift reaction). In practical onboard applications, fuel reforming may be accomplished using EGR as the source of steam and enthalpy. For more details about fuel reforming and its application on board vehicles, see references [3] to [6].

H_2 is an alternative energy carrier which produces non-toxic gases when combusted in air. The density of H_2 is one order of magnitude lower than that of NG, which makes it an undesirable fuel for mobile applications. H_2 has a wider flammability limit than NG, especially on the lean side. Its autoignition temperature is higher than that of NG, which makes it theoretically a higher-octane fuel. However, the low minimum ignition energy of H_2 reduces its superb resistance to autoignition in practical systems. The lower heating value of H_2 is three times that of NG, but its low density and high air-to-fuel ratio reduces the energy-carrying capacity of H_2 at a similar air-to-fuel ratio compared with NG. Hence, H_2 enrichment of NG-fuelled SI engines is not expected to lead to an increase in engine power under similar conditions.

1.2 Previous research

H_2 or RG enrichment has been studied for many years. The early studies investigated the effect of H_2 enrichment on flames under standard temperature and pressure conditions, and later under elevated pressures and temperatures that simulate actual

Table 1 Combustion-related properties of NG, H_2, CO, and gasoline from reference [2]

Property	Value for the following			
	H_2	CO	NG	Gasoline
Density (kg/m^3)	0.0824	0.789	0.72	730
Flammability limit (vol% in air)	4–75	12.5–74	4.3–15	1.4–7.6
Flammability limit φ	0.1–7.1	0.3–6.8	0.4–1.6	≈ 0.7–4
Autoignition temperature in air (K)	858	609	723	550
Minimum ignition energy (mJ)	0.02	< 0.30	0.28	0.24
Flame velocity (m/s)	1.85		0.38	0.37–0.43
Adiabatic flame temperature (K)	2480		2214	2580
Quenching distance (mm)	0.64		2.1	≈ 2
Stoichiometric air-to-fuel ratio	34.48	2.46	14.49	14.70
Lower heating value (MJ/kg)	119.7	10.1	45.8	44.79
Heat of combustion (MJ/(kg air))	3.37	4.1	2.9	2.83

internal combustion engine conditions. These studies have focused on flame development using both stationary combustion chambers and internal combustion engines.

One group of H_2 enrichment studies focused on the burning velocities of flames. The laminar burning velocities of binary and tertiary mixtures of H_2, CO, and methane (CH_4) were studied in a fundamental experimental study by Scholte and Vaags [7]. Rauckis and McLean [8] operated a Waukesha Co-operative Fuel Research (CFR) engine with up to 30 per cent H_2 enrichment. It was found that H_2 enrichment primarily affects the ignition delay (or flame kernel growth). Heywood and Vilchis [9] reported that the H_2 enrichment effect was primarily on the rapid initial flame development (mostly controlled by the laminar flame speed) and a faster (by a factor of 2) fully developed turbulent flame. Recently Halter et al. [10] found that H_2 enhanced small-scale flame front wrinkling in the turbulent zone.

Milton and Keck [11] found that a double-peak burning velocity behaviour of H_2 enriched the propane flame with increasing pressure using a constant-volume combustion chamber. Rafael and Sher [12] tried to explain the double-peak behaviour of the flame speed that was observed by Milton and Keck using a numerical model with 169 elementary reactions and complex H_2 oxidation mechanisms.

Yu et al. [13] defined a parameter for H_2 enrichment based on mixture molar ratios. They found that increasing the H_2 enrichment parameter leads to a linear increase in the laminar burning velocity of the mixture. Recently studies by Coppens et al. [14], Mandilas et al. [15], and Di Sarli and Benedetto [16] examined the effect of H_2 on the laminar burning velocities of CH_4, both experimentally and numerically.

A second group of studies investigated the knock characteristics of H_2, CO, and their blends with conventional fuels. Rafael and Sher [17] found that H_2 retarded the autoignition of n-butane owing to a reduction in the OH concentration in the second stage of reactions that provides OH for the main combustion stage. Li et al. [18] found that the excellent knock resistance property of CO deteriorated significantly with the presence of small amounts of H_2, CH_4, or H_2O. Hence, it is not expected that RG will not benefit from the high knocking resistance of dry CO owing to the presence of H_2O in the recirculated exhaust gases. Li and Karim [19] found that CH_4 addition is more effective than CO addition for improving the knocking resistance characteristics in a H_2-fuelled SI engine. They also found that H_2 addition did not significantly affect NO_x emissions near stoichiometric conditions, but that NO_x emissions increased significantly when the mixture became lean [20]. Topinka et al. [21] found that RG (H_2–CO mixture) inhibited knock by slowing the autoignition chemistry and by slightly increasing the flame speed. They assumed octane numbers of 106 and 140 for CO and H_2 respectively. They estimated that, if 15 per cent of the primary reference fuel is converted to RG, the octane number of the resulting fuel will be approximately ten numbers higher.

A third group of studies focused on SI engine performance and emissions under H_2-enriched conditions. Nagalingam et al. [22] found that H_2 enrichment decreased power and efficiency and increased NO_x emissions at constant air-to-fuel ratio and no EGR. Karim et al. [23] noted that CH_4 replacement with H_2 leads to reduced energy delivery at constant intake conditions since CH_4 has 54 per cent more energy content at stoichiometric conditions. H_2-enriched combustion increased the H_2O content of the residual gases, improving power and efficiency owing to a faster flame speed, reduced combustion duration, and optimized combustion timing, especially in lean conditions, reduced emissions of CO, CH_4, and CO_2, and increased NO_x emissions.

Isherwood et al. [24] decreased engine start-up emissions, replacing RG for HC by 80 per cent and CO by 40 per cent. Shrestha and Karim [25] reported an optimum value of 20–25 vol % for H_2 enrichment of a CH_4-fuelled SI engine. This suggests that only a small amount of H_2 is needed to improve SI engine performance to compensate for flame depletion under lean combustion conditions. Kirwan et al. [26] reported that using partial oxidation products significantly reduced HC emissions during cold starting and reduced the catalyst warm-up period considerably. Blending gasoline with 30 per cent partial oxidation reforming products reduced NO_x emissions by between 55 and 85 per cent by increasing the EGR limit. Smith and Bartley [27] reported the EGR tolerance enhancement of an NG SI engine to be 44 per cent more than the baseline case. They utilized the synthesis gas in the EGR system by using a partial oxidation CH_4 catalyst. Allenby et al. [28] investigated the potential to expand the EGR limit of an NG-fuelled SI engine using reformer products (H_2 and CO) of an exhaust catalytic fuel processor. It was found that for indicated mean effective pressures (IMEP) between 2 and 4 bar and 25 per

cent EGR at fixed combustion timing, 5–25 per cent H_2 in the EGR stream was required (depending on the load) to maintain the combustion cyclic variations (as measured by the coefficient of variation (COV) of IMEP) below 5 per cent. Bauer and Forest [29, 30] used the CFR engine and reported that increasing the H_2 fraction by up to 60 vol % decreased the brake-specific CO_2 by 26 per cent, brake-specific CO by 40 per cent, and brake-specific HC by 60 per cent, and increased brake-specific NO_x by 30 per cent. During simulating driving cycles, it was found that there is an optimum range of H_2 enrichment that benefits both urban and the highway driving cycles for maximum efficiency and minimum emissions.

Kirwan et al. [31] reported a decrease of 75 per cent in HC emissions using RG during cold starting. Tunestål et al. [32] found that H_2 is more effective when used in slower combustion chamber designs than in faster designs. Quader et al. [33] found that RG enhances the lean limit from $\varphi = 0.7$ to $\varphi = 0.4$ (44 per cent leaner) and EGR tolerance from 15 per cent to 37 per cent (115 per cent higher) while keeping $COV_{imep} < 3$ per cent. It was found that EGR limit expansion is a more effective strategy than lean limit expansion. Tully and Heywood [34] used a plasmatron fuel reformer to study the effect of reformer gas addition to a gasoline SI engine. The study found that using plasmatron fuel reformer increases the fuel conversion efficiency by up to 12.3 per cent. In a recent study by Allgeier et al. [35], an SI engine was operated in all modes using gasoline enriched with reformer gas produced by partial oxidation. The strategy was to use reformer gases to achieve near-zero HC emissions during cold starting, and excess air to produce a highly exothermal reaction that enhanced catalyst warm-up, and finally to use a certain amount of reformer gases under low and medium loads to increase efficiency and to reduce NO_x emissions.

Czerwinski and Comte [36] examined the effect of RG on the performances of two small gasoline SI engines. They reported an EGR limit expansion from 7 per cent to 55 per cent and lean limit (relative air-to-fuel ratio) expansion from $\lambda = 1.1$ to $\lambda = 2.55$. Alger et al. [37] found that adding 0.2 per cent and 0.4 per cent H_2 to the intake system improved the EGR limit to 20–28 per cent and 40–45 per cent respectively.

In addition to the H_2 enrichment studies, the operating characteristics and performance of dedicated H_2-fuelled SI engines were investigated by Karim [38] and White et al. [2].

1.3 Current objective

The objective of the current study was to investigate the use of RG to reduce NO_x emissions from an NG SI engine while maintaining high fuel conversion efficiency. The focus was on expansion of the EGR dilution limit; hence the research is considered complementary to that by Rauckis and McLean [8], who altered the air-to-fuel ratio using excess air. In this study, the air-to-fuel ratio was kept constant ($\lambda = 1$), but the EGR dilution was increased. This paper examines the effects of simulated RG enrichment on the performance characteristics of a relatively high-compression-ratio NG-fuelled SI engine operated with a stoichiometric mixture to enable the use of the TWC and different levels of EGR dilution.

2 EXPERIMENTAL SET-UP

All experiments were conducted in a single-cylinder CFR engine. The CFR engine is suitable for investigating different combustion strategies, but it should be noted that this engine has very high internal friction and a limited upper speed range. Table 2 shows the CFR engine's specifications and operating conditions for this study.

Figure 1 is a schematic diagram of the gaseous fuels supply system. NG was supplied from a high-pressure tank that was filled regularly by ATCO Gas in Edmonton. The natural gas composition on a molar basis was 95.39 per cent CH_4, 1.90 per cent ethane (C_2H_6), 1.93 per cent N_2, and 0.78 per cent oxygen (O_2). An alternative fuel system (AFS) (model Falcon) electronic double-stage regulator R2 was used to provide a constant NG pressure (80 lbf/in²g (551.5 kPa)) in the delivery line.

Simulated RG with 75 per cent H_2 and 25 per cent CO on a volume basis was provided from Praxair high-pressure tanks. The RG pressure in the supply line was adjusted manually using a double-stage

Table 2 Waukesha CFR engine specifications and operating conditions

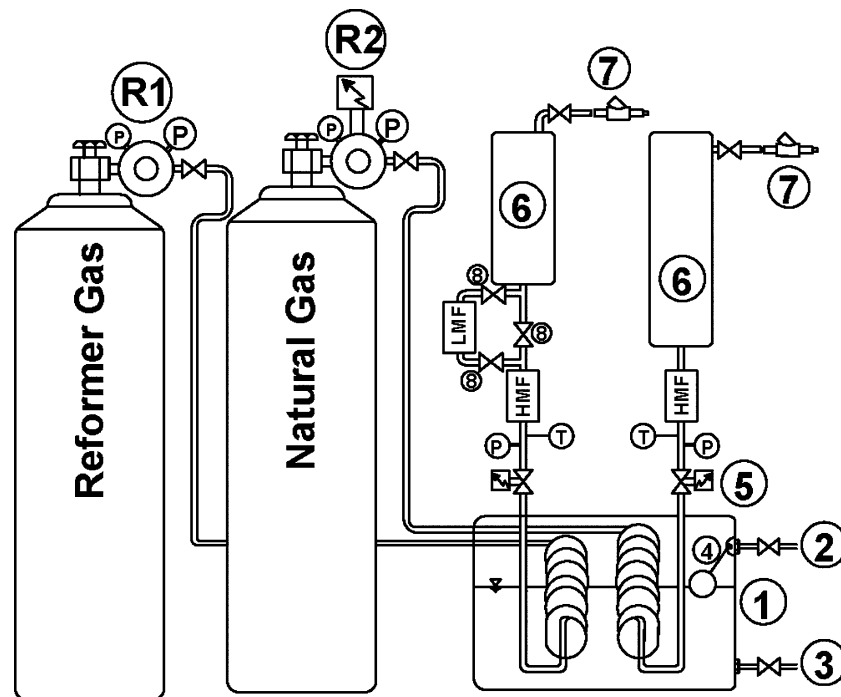| Engine parameter	Description or value
Combustion chamber	Pancake, flat-top piston
Compression ratio	11.5, constant
Displacement (cm³)	612
Bore (mm)	82.6
Stroke (mm)	114.3
Engine speed (r/min)	1200 constant
Throttle	Wide open, naturally aspirated
Spark timing (deg crank angle (CA))	Maximum for best torque (MBT) (limited to range from −45° to top dead centre (TDC))

Fig. 1 NG and RG supply system

pressure regulator R1. The RG pressure was kept constant at 95 lbf/in²g (655 kPa).

The NG and RG feed lines were routed through a liquid–gas heat exchanger 1. Warm building water was supplied to the heat exchanger 2 and was drained continuously 3 to keep the NG and RG temperatures constant at 35 °C. The NG line was equipped with a high-mass flowmeter (HMF) calibrated in the range 0–50 standard l/min. The RG line was equipped with a low-mass flowmeter (LMF) and an HMF to ensure maximum accuracy of RG mass flow measurement. The flowmeters were calibrated in the ranges 0–5 standard l/min and 0–50 standard l/min respectively. A series of Swagelok stainless steel ball valves was used to switch the flow between the two mass flowmeters. Two pressure-rated vessels 6 were used downstream of the flowmeters and upstream of the injectors to dampen the injection pressure waves in the fuel delivery lines. The AFS gaseous fuel injectors were used to deliver both NG and RG to the intake plenum.

Figure 2 is a schematic diagram of the main experimental hardware. The NG and RG injectors 7 were installed in the intake plenum 8 of the CFR engine 9. A hot-wire anemometer 10 was used to measure air mass flowrates. A 220-l drum 11 was installed in the intake system to dampen air pulsations. The throttling valve 12 was kept wide open during experiments. EGR flow 14 was initiated by restricting the exhaust with a back pressure valve 12 and controlled using an EGR valve 15.

Gas analysers manufactured by Analytical Instruments were used to measure the NO_x, HC, CO, CO_2, and O_2 exhaust emissions. The EGR level was defined as the ratio of CO_2 volumetric concentration in the intake to that in the exhaust. The CO_2 analyser was also used to measure the CO_2 concentration in the intake plenum to quantify the EGR rate.

National Instruments' data acquisition hardware and software (Labview^TM) were used to acquire experimental data. Engine mean operating parameters were collected on a cycle basis and were averaged over the entire cycle (flowrate, pressure, and temperature). A Kistler 6043A water-cooled pressure transducer was used to measure the cylinder pressure. The pressure trace was collected with 0.1° crank angle resolution for 100 consecutive cycles in raw voltage format. MATLAB® was used to calibrate reference and filter noise from the pressure traces. The Rassweiler–Withrow method [39] was applied to compute the mass fraction burned using the PTrAn software package supplied by Optimum Power Technology. The measurement error bars in the figures calculated using an external error analysis technique represent 95 per cent confidence intervals ($\pm 2\sigma_{n-1}$).

Since the RG (75 per cent H_2 and 25 per cent CO) contains O_2, the relative air-to-fuel ratio λ was
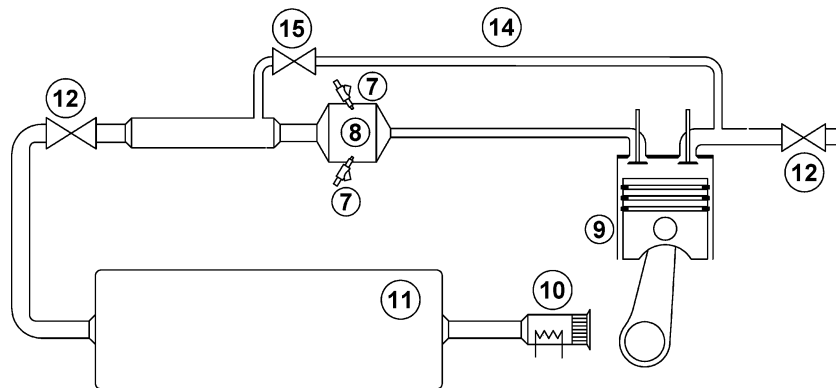
Fig. 2 Schematic diagram of the main experimental set-up hardware

calculated using the chemical valences of the reactants (C, +4; H, +1; O, −2; N, 0) considering both NG and RG as fuels. The RG mass fraction was calculated using

$$\text{RG mass } (\%) = \frac{100\dot{m}_{\text{RG}}}{\dot{m}_{\text{RG}} + \dot{m}_{\text{NG}}}$$

The experiments were conducted in the steady state conditions with an engine speed $N = 1200$ r/min, wide-open throttle (WOT) at atmospheric intake pressure, MBT spark timing, and a stoichiometric air-to-fuel ratio ($\lambda = 1$). The NG flowrates were adjusted during the experiments as the EGR fraction and RG blending were varied to keep $\lambda = 1$ constant.

Based on Heywood's [**40**] definition, MBT spark timing was considered to be the operating point where the IMEP is maximum, subject to the requirement that the COV$_{\text{imep}}$ is acceptable. Since the spark timing's reading was made with a stroboscope light and scale on the flywheel and the torque curve at constant speed near TDC is quite flat [**40**], it is estimated that the tolerance associated with the MBT spark timings is $\pm 2°$ CA.

3 RESULTS AND DISCUSSION

3.1 Natural gas baseline

As the engine speed (= 1200 r/min) and λ (= 1) were kept constant during the experiments, baseline engine operation fuelled by NG was affected only by the spark timing and EGR fraction. Figure 3 shows that the IMEP increased as the spark timing was advanced up until the knock limit when the EGR level of 0 per cent was encountered. In order to operate with further advanced spark timings, increasing levels of EGR had to be applied, which

eventually led to much higher cyclic variations in IMEP.

Figure 4 shows that the IMEP decreased and the COV$_{\text{imep}}$ increased with increasing EGR level while maintaining the MBT spark timing. As expected, more advance spark timings were required to keep the combustion timing optimal at higher EGR levels.

Figure 5 shows that there is a nearly linear decrease in NO$_x$ emissions as the EGR level is increased. Moreover, indicated specific fuel consumption and CO emissions also decreased when the EGR level was increased to 8 per cent. The experimental data suggest that there is a maximum tolerance to an EGR level of 12 per cent for these operating conditions. There is a sharp increase in
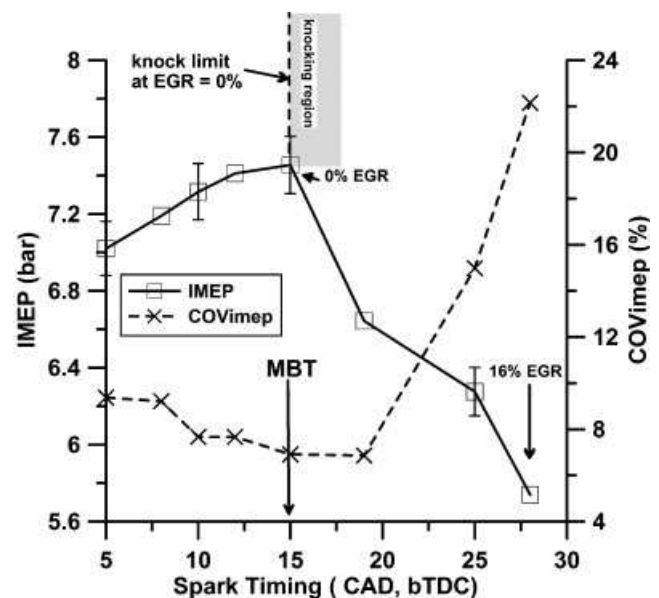

Fig. 3 Effect of spark timing on the engine's IMEP and COV$_{\text{imep}}$ (base-line test: CFR engine; compression ratio, 11.5; $N = 1200$ r/min; EGR level, 0–16 per cent; $\lambda = 1$; dedicated NG) (CAD, bTDC, degrees crank angle before top dead centre)
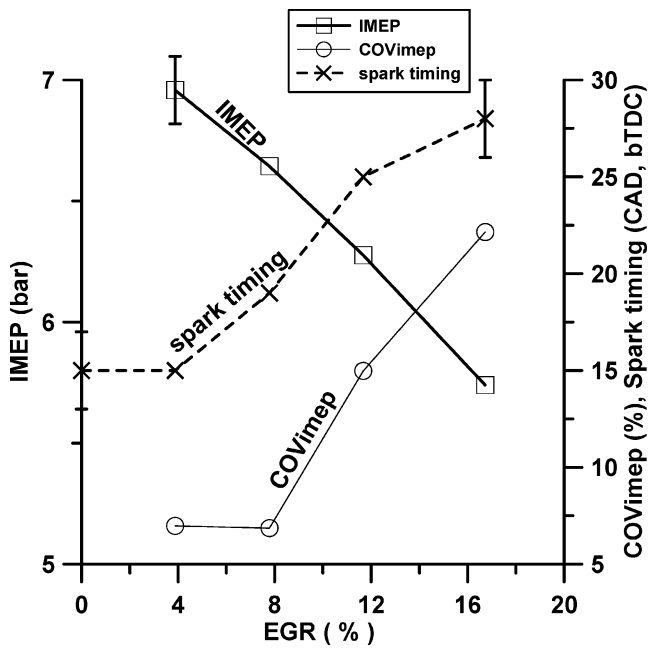
Fig. 4 Effect of the EGR level on the IMEP, COV_{imep}, and MBT (base-line test: CFR engine; compression ratio, 11.5; $N = 1200$ r/min; $\lambda = 1$; dedicated NG) (CAD, bTDC, degrees crank angle before top dead centre)

HC and CO emissions, as well as indicated specific fuel consumption, as a result of the reduced burning velocity, retarded combustion timing, and low
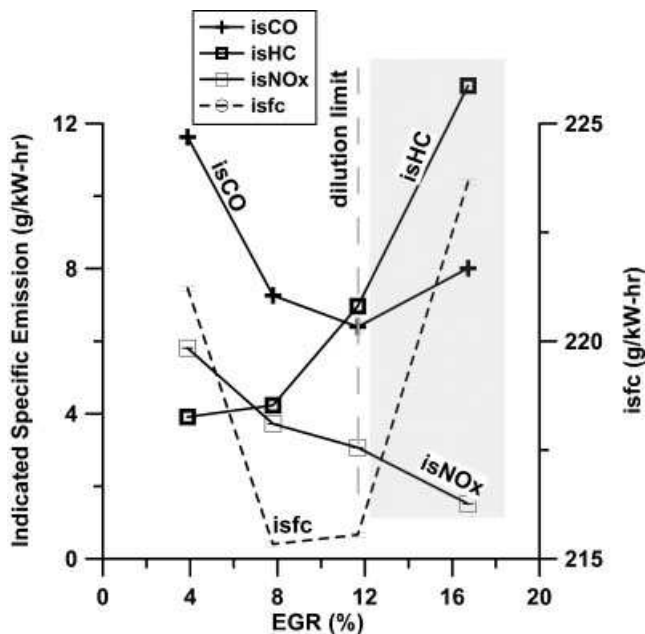

Fig. 5 Effect of the EGR level on the indicated specific (is) emissions and indicated specific (fuel consumption (isfc)) (base-line test: CFR engine; compression ratio, 11.5; $N = 1200$ r/min; $\lambda = 1$; dedicated NG)

combustion temperatures that occur at high levels of EGR when the engine is operated with NG.

3.2 RG blending: operating region

The CFR engine was operated using NG blended with various RG mass fractions and EGR rates while keeping an overall stoichiometric air–fuel mixture. The spark timing was adjusted for MBT at each operating point. The RG–EGR operating range obtained from all experimental data points is shown in Fig. 6.

As indicated in the previous section, the EGR dilution limit for baseline operation with NG was 12 per cent EGR. Figure 6 shows that increasingly higher levels of EGR can be tolerated as the RG mass fraction increases. However, the limit for EGR dilution was found to be 40 per cent, beyond which reasonable combustion stability could not be achieved with any level of RG.

The spark timing adjustment system on the CFR engine used in this study was limited to spark timings before TDC. However, the MBT spark timing becomes more retarded as the RG mass fraction is increased at a given EGR level, as shown in Fig. 7. Thus, the current experiments were limited to conditions where the MBT spark timing occurred up to TDC. Beyond that, further increases in RG were not possible because the engine could not be retarded to the MBT spark timing.
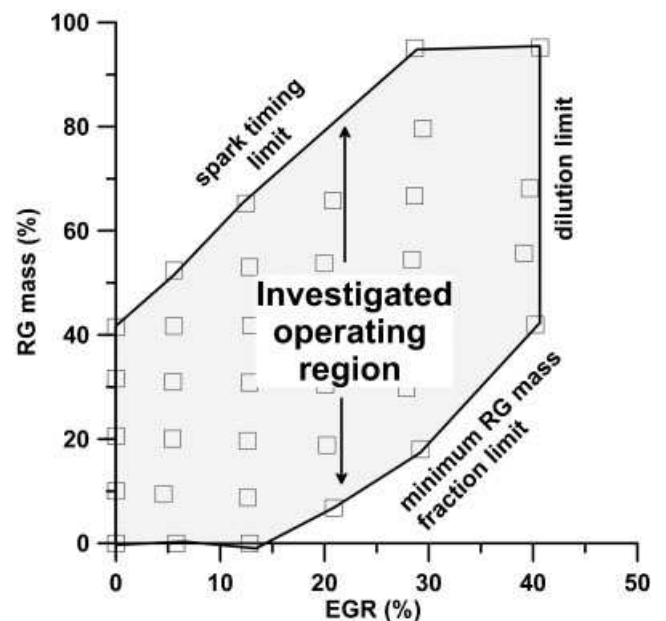

Fig. 6 The engine's EGR–RG operating map (CFR engine; compression ratio, 11.5; $N = 1200$ r/min; $\lambda = 1$; RG-blended NG)
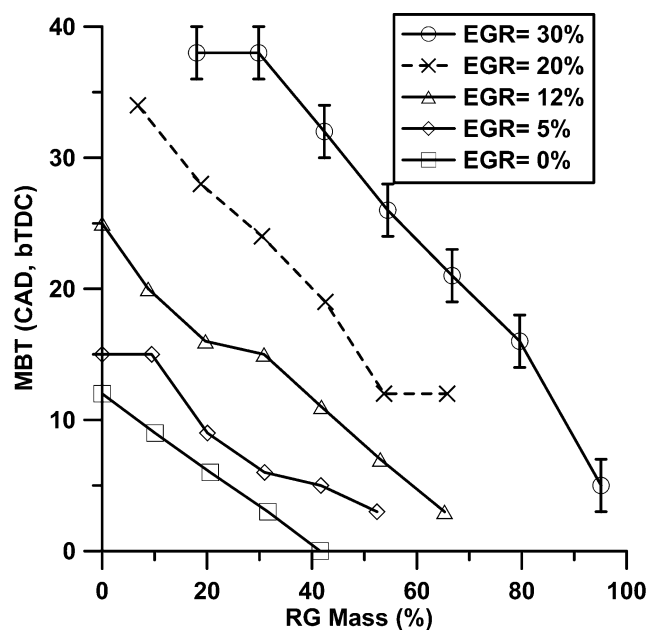

Fig. 7 Effect of increasing the RG on the MBT spark timing (CFR engine; compression ratio, 11.5; $N = 1200$ r/min; $\lambda = 1$; RG-blended NG)

Fig. 8 Effect of increasing the RG on the IMEP (CFR engine; compression ratio, 11.5; $N = 1200$ r/min; $\lambda = 1$; RG-blended NG)

The RG mass fraction was increased to slightly less than 100 per cent during the experiments, where possible. However, an RG mass fraction of 30–35 per cent is reasonable. Figure 6 shows that increasing the RG mass fraction from 0 per cent to 35 per cent increased the EGR tolerability of the engine from 12 per cent to 35 per cent.

3.3 RG enrichment: engine performance

There was no expectation that RG addition would increase the IMEP significantly because the volumetric energy density of RG is much lower than that of NG and the mixture stoichiometry was held constant. Any observed IMEP improvement would be due to improved combustion stability, more optimized combustion timing, or less flame kernel depletion at highly diluted conditions.

Figure 8 shows that the IMEP increased slightly at lower RG levels for EGR levels up to 30 per cent. As the EGR level increased, the appropriate RG mass fraction required to optimize IMEP was also found to increase. If more than the optimal RG fraction was added, the IMEP decreased gradually. The experimental data also indicate that it is possible to operate the engine at WOT over the IMEP range 4.5–7 bar with an appropriate level of EGR and with RG addition.

Figure 9 shows that, for EGR levels of 0–30 per cent, RG addition reduced the combustion instability, as measured by COV_{imep}. For EGR levels below 12
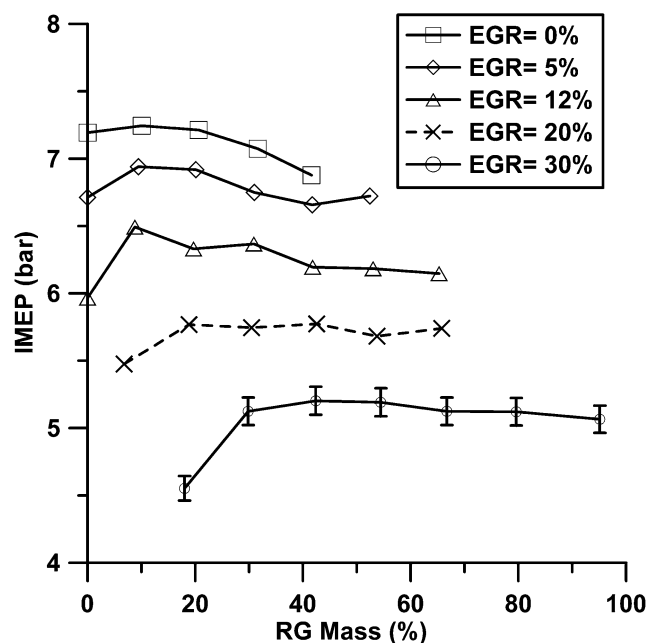
per cent, RG addition reduced the cyclic variations in IMEP. The RG addition was required to maintain acceptable combustion stability above 12 per cent EGR. Beyond 40 per cent EGR, acceptable combustion stability could not be achieved with any level of RG addition. This is probably due to the relatively
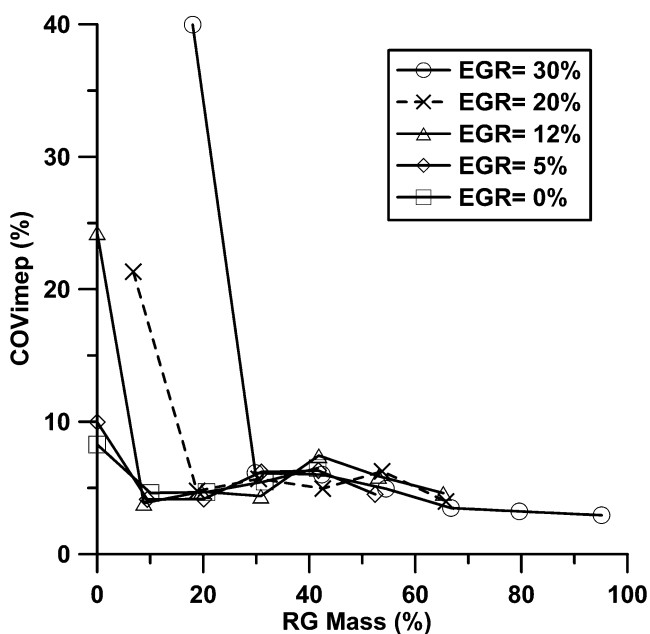

Fig. 9 Effect of increasing the RG on the COV_{imep} reduction (CFR engine; compression ratio, 11.5; $N = 1200$ r/min; $\lambda = 1$; RG-blended NG)

quiescent conditions inside the combustion chamber of the CFR engine and not the combustion phenomenon itself. This engine experiment was not set up with particular consideration of fuel–air–EGR mixing or charge stratification around the spark plug. At high EGR rates, the combination of a highly diluted mixture and the high octane numbers of NG, H_2, and CO, as well as no charge stratification inside the combustion chamber, led to unacceptable combustion stability. However, it should be noted that with RG addition and EGR levels of 30–40 per cent, the cyclic variations were lower than those measured for baseline engine operation with NG.

The indicated fuel conversion efficiency is plotted as a function of RG mass fraction and EGR level in Fig. 10. For each EGR level, there is a desirable level of RG addition to optimize the indicated fuel conversion efficiency. The maximum efficiency points are shown in the banded region of the figure. As expected, the optimal RG addition to reduce IMEP cyclic variations and to optimize the combustion timing increases with increasing EGR level.

Figure 10 shows that increasing EGR level leads to higher indicated thermal efficiency independent of the RG. Use of EGR raises the wall temperatures during the intake and compression strokes as well as reducing peak combustion temperature. As described by Heywood [40], these effects reduce expansion stroke heat losses and increase indicated combustion efficiency,
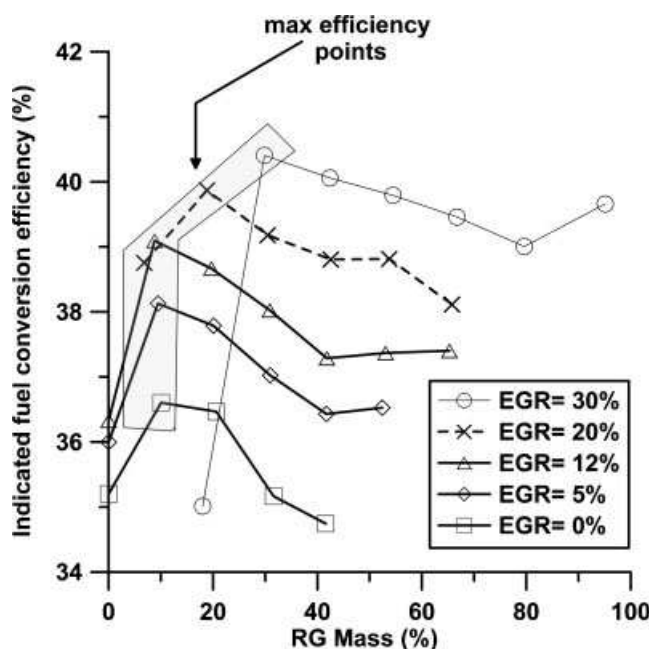
provided that the EGR quantity is not sufficient to affect the combustion stability and duration severely. However, the combustion stability and burning velocity degrade when higher levels of EGR are used without RG. For example, use of 20 per cent EGR required 10 per cent RG to stabilize ignition and use of 20 per cent RG to speed combustion sufficiently for optimum thermal efficiency. The degradation of indicated fuel conversion efficiency for greater RG blend fractions greater than optimum may be attributed to increased heat losses due to the heat transfer contribution of hydrogen and water vapour.

The indicated fuel conversion efficiency is significantly affected by apparent combustion efficiency, and engine output is further affected by volumetric efficiency. The combustion efficiency accounts for losses due to unburned fuel or incomplete combustion, while the volumetric efficiency accounts for losses that occur during the gas exchange processes. RG addition effects on the combustion and volumetric efficiencies for experiments conducted with nominal 30 per cent EGR are indicated in Fig. 11. For the 30 per cent EGR case, 20 per cent RG was required to achieve reliable ignition but the figure shows that increasing the RG level from 20 per cent to 30 per cent raises the combustion efficiency from 92 per cent to 95 per cent. Further RG addition did not have a significant effect on combustion efficiency. On the other hand, the volumetric efficiency was quite low because of the 29 per cent EGR employed. The volumetric efficiency decreased monotonically with increasing

Fig. 10 Effect of increasing the RG on the fuel conversion efficiency (CFR engine; compression ratio, 11.5; $N = 1200\,\text{r/min}$; $\lambda = 1$; RG-blended NG)
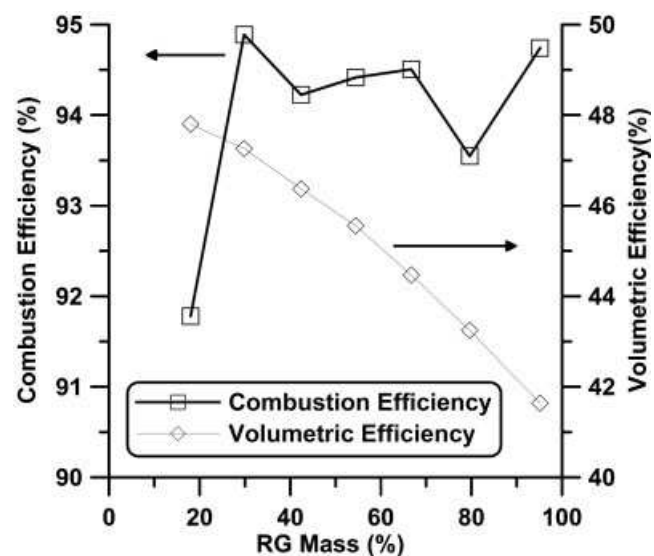

Fig. 11 Effect of the RG on the combustion efficiency and volumetric efficiency (EGR level, 28.8 ± 0.7 per cent; $\lambda = 0.99 \pm 0.02$)

RG blend fraction. The gas exchange loss continuously increases with increasing RG blend fraction because of the reduced ability of the engine to draw air when NG is replaced with lower-density RG.

3.4 RG enrichment: combustion analyses

The cylinder pressure data were analysed to investigate the effect of RG addition on the combustion process for the data points with an EGR level of 28.8 ± 0.7 per cent and $\lambda = 0.99 \pm 0.02$. The RG blend fraction covered the wide range 18.0–95.1 per cent.

Figure 12 shows the effect of RG mass fraction on the combustion events as determined using a mass fraction burn (MFB) analysis of the cylinder pressure data. This figure shows the MBT spark timing, as well as the location of the 10 per cent MFB (CA10), 50 per cent MFB (CA50), and 90 per cent MFB (CA90). Increasing the RG blend fraction at constant initial conditions (constant EGR fraction and constant λ) significantly retarded the MBT spark timing but did not have a large effect on the timing of the CA10, CA50, and CA90 combustion phasing. However, the ignition delay between the spark timing and the CA10 combustion event was reduced significantly as the RG blen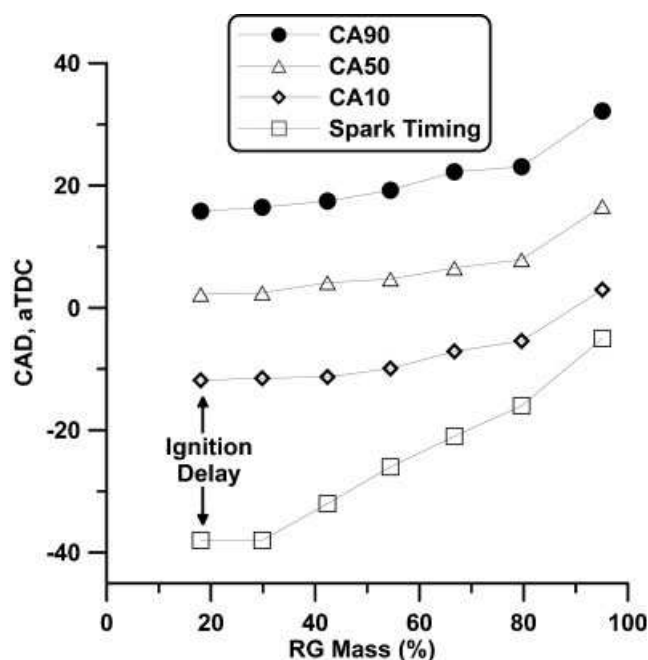d fraction increased. The combustion duration, if defined as the CA difference between CA10 and CA90, was fairly constant over the wide range of RG blend fractions investigated. This result confirms the observations in earlier fundamental studies that H_2 enhances the flame kernel development stage but does not significantly affect the fully developed turbulent flame speed.

Comparing the two cases with RG mass fractions of 18 per cent and 29 per cent, the mean ignition delays were not significantly different. However, the combustion stability was greatly enhanced, which led to a more consistent combustion event from cycle to cycle. This is manifested in smaller error bars in the timings of the various combustion events and reduced cyclic variations in the IMEP, as shown previously in Fig. 9.

3.5 RG enrichment: emissions

So far, it has been demonstrated that RG enrichment extends the EGR limits for an NG-fuelled SI engine and increases combustion stability. It is well known that EGR is a relatively simple way to reduce the peak temperatures inside the combustion chamber for the purposes of significantly reducing NO_x emissions. Figure 13 demonstrates the use of RG enrichment to enable an SI engine to operate at high EGR rates with extremely low NO_x emissions.

Fig. 12 Effect of the RG on the combustion events of spark timing (SI) (CA10, CA50, and CA90; EGR level, 28.8 ± 0.7 per cent; $\lambda = 0.99 \pm 0.02$) (CAD, aTDC, degrees crank angle after top dead centre)
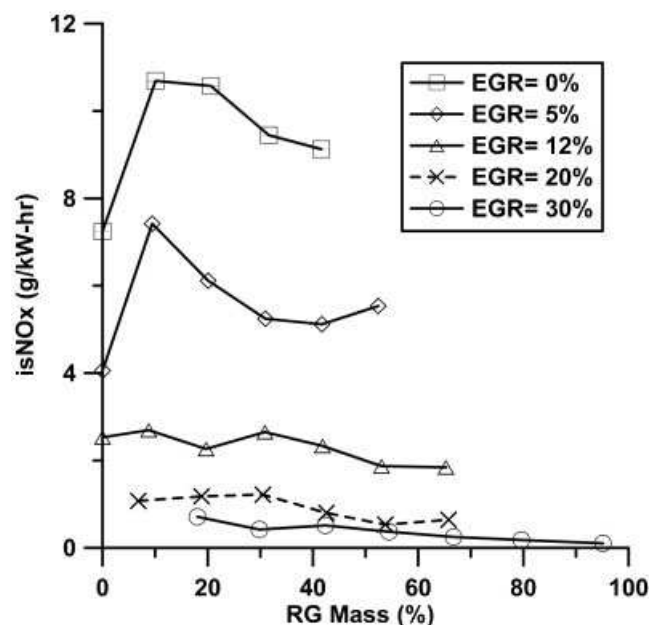

Fig. 13 Effect of increasing the RG on the indicated specific (is) NO_x emissions (CFR engine; compression ratio, 11.5; $N = 1200$ r/min; $\lambda = 1$; RG-blended NG)

Figure 13 shows that the baseline NO_x emissions without EGR for the SI engine fuelled with NG under the prescribed conditions were greater than 7 g/kW h. RG addition allowed the engine to be operated with 30 per cent EGR, which reduced the NO_x emissions by roughly one order of magnitude, depending on the RG mass fraction.

One of the challenges associated with the use of EGR is an increase in unburned HC emissions. Figure 14 shows that HC emissions increase from 4 g/kW h to around 8 g/kW h for the operating region of 20–30 per cent EGR and 20–30 per cent RG mass fraction, even though the spark timing was adjusted for MBT. Higher EGR rates reduce combustion temperatures and lower the late-cycle HC oxidation rate.

Figure 14 also shows that RG addition tends to compensate somewhat for the HC emission increase associated with EGR. This is a natural result of reducing the carbon content of the fuel by adding a more hydrogenated fuel component (in this case, RG). The increase in the H-to-C ratio of the fuel that results from RG addition leads to a reduction in the HC emissions.

The effect of EGR and RG addition on CO emissions is shown in Fig. 15. The CO emissions were found to decrease as the RG mass fraction increased from 0 per cent to 20 per cent. This is believed to be due to improvements in the combustion stability as the RG mass fraction increases. However, CO emissions tend

Fig. 15 Effect of increasing the RG on the indicated specific (is) CO emissions (CFR engine; compression ratio, 11.5; $N = 1200$ r/min; $\lambda = 1$; RG-blended NG)

to increase for RG mass fractions greater than 20 per cent. This may be due to the higher CO content of the fuel and increased quenching of the CO-to-CO_2 oxidation reaction as the RG mass fraction increases. It may also be due to CO present in the RG
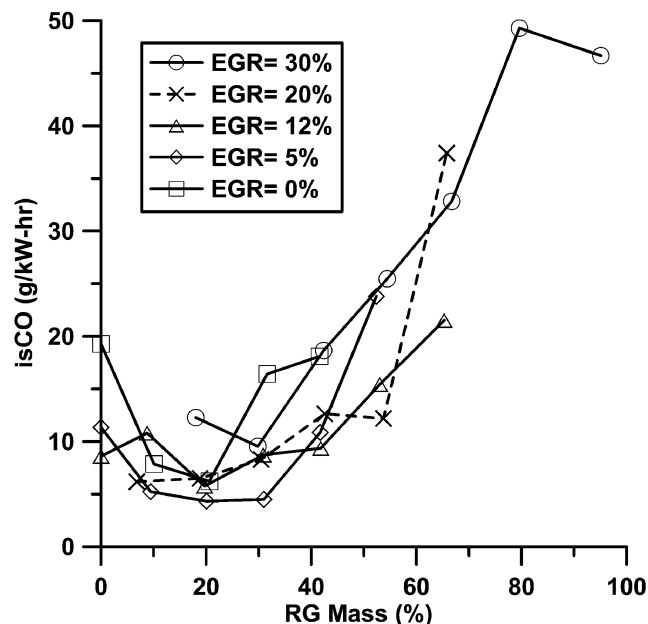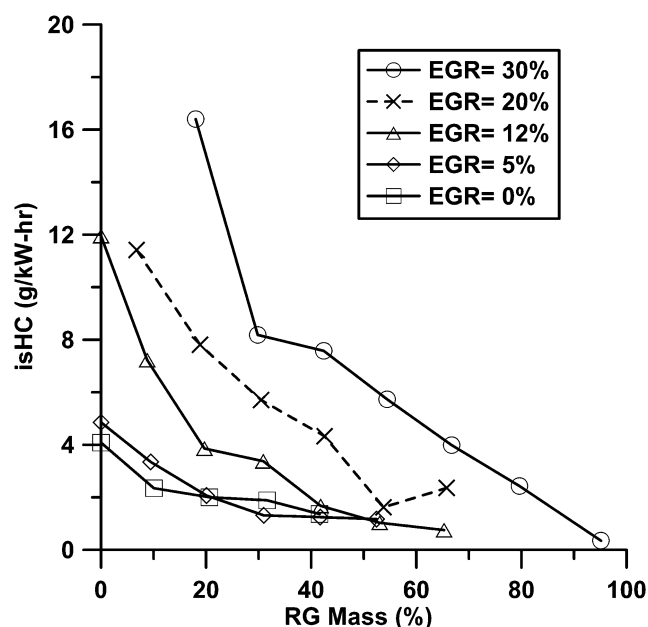

Fig. 14 Effect of increasing the RG on the indicated specific (is) HC emissions (CFR engine; compression ratio, 11.5; $N = 1200$ r/min; $\lambda = 1$; RG-blended NG)
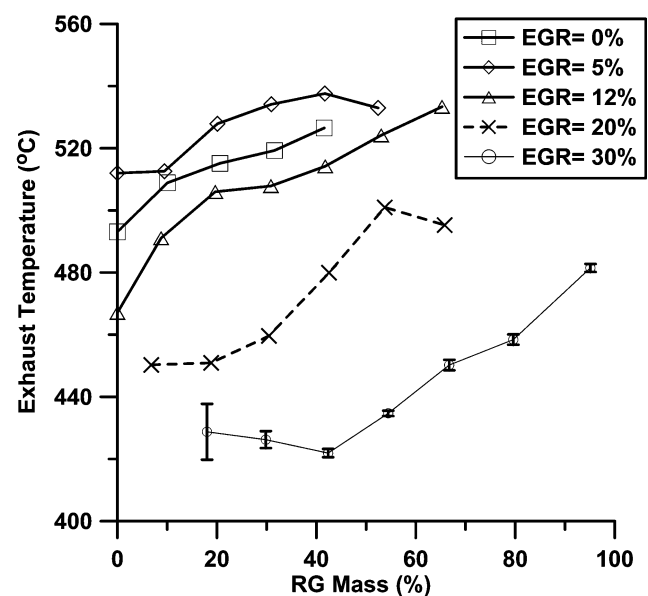

Fig. 16 Effect of increasing the RG on exhaust temperature (CFR engine, compression ratio, 11.5; $N = 1200$ r/min; $\lambda = 1$; RG-blended NG)

(25 mass %) which finds its way into the exhaust stream during the valve overlap period.

3.6 Efficiency–emissions trade-off

The objective of this study was to investigate the addition of partially reformed NG into an NG-fuelled SI engine to extend the EGR limit and to reduce NO_x emissions. The engine was operated under stoichiometric conditions assuming that a TWC would also be used to reduce NO_x, HC, and CO emissions further. In this section, this strategy will be assessed in terms of NO_x emission reduction and its impact on overall system efficiency.

For discussion purposes, the NO_x emissions will be compared with the EPA standard of 0.2 g/bhp h for heavy-duty highway engines for model year 2007 and later. The equivalent indicated specific NO_x emissions standard in SI units would be approximately 0.22 g/kW h, assuming a 20 per cent loss in going from indicated to brake power values.

Figure 13 shows that the baseline NO_x emissions of 7 g/kW h can be reduced to approximately 0.5 g/kW h by adding 30 per cent mass fraction RG, which enables operation with 30 per cent EGR. The exhaust gas temperature under these conditions is approximately 425 °C, as shown in Fig. 16. A TWC should have an NO_x reduction efficiency of approximately 80 per cent under these conditions. This should enable NO_x emissions of 0.1 g/kW h to be achieved, which would meet the 2007 EPA emission standard for heavy-duty engines with a reasonable margin of safety.

If attention is switched to overall system efficiency, Fig. 10 shows that the indicated specific fuel conversion efficiency increases from 35 per cent to 40 per cent by the use of 30 per cent RG mass fraction and 30 per cent EGR. This corresponds to a 14 per cent increase in fuel conversion efficiency. On the other hand, the generation of 30 per cent RG mass fraction with an 80 per cent efficient fuel reformer will suffer from a 6 per cent reduction in efficiency. Since the increase in fuel conversion efficiency is greater than the loss in efficiency due to fuel reforming, it is reasonable to assume that the fuel reforming process will not lead to a compromise in the overall engine efficiency while achieving NO_x emissions below 0.2 g/kW h owing to the extended EGR limit.

In summary, the approach of using fuel reforming to extend the EGR limit of an NG-fuelled SI engine appears to be a potentially attractive method for reducing NO_x emissions below 0.2 g/kW h without compromising the fuel conversion efficiency of the engine.

4 CONCLUSIONS

Simulated reform gas enrichment (75 per cent H_2 and 25 per cent CO) to expand the EGR limit and to reduce NO_x emissions from an NG-fuelled SI engine was investigated. The effects of RG enrichment and EGR dilution on the performance, combustion behaviour, and emissions from a CFR engine operated with stoichiometric fuel–air mixtures, to enable the use of the TWC, were reported.

When the engine was fuelled with NG, the maximum EGR tolerance was 12 per cent owing to retarded combustion timing and excessive cyclic variations in the combustion process. The addition of RG expanded the maximum EGR tolerance to approximately 40 per cent. Engine-out indicated specific NO_x emissions below 1 g/kW h were typically achieved when the RG blend fraction and EGR levels were greater than 20 per cent. The NO_x emissions could be further reduced to meet a stringent future standard (e.g. the US EPA 2007 emissions standard for on-highway heavy-duty diesel engines) using a TWC. The TWC is needed to oxidize the higher HC emissions produced with increasing EGR level.

Increasing the RG blend fraction at constant initial conditions (constant EGR fraction and constant λ) significantly retarded the MBT spark timing but did not have a large effect on the timing of the CA10, CA50, and CA90 combustion phasing. However, the ignition delay between the spark timing and the CA10 combustion event was reduced significantly as the RG blend fraction increased.

The optimal RG fraction was found to be just enough to compensate the decrease in the burning velocity due to the EGR level and to return it to the normal values. Adding more RG than the minimum requirement for combustion enhancing caused a penalty in the power and efficiency of the engine.

Overall, a simple energy balance showed that the fuel conversion efficiency increases if an optimal combination of EGR level and RG enrichment is used, which more than compensates for the assumed 20 per cent loss of energy associated with the fuel reforming process.

and the Government of Canada's Program for Energy Research and Development (PERD/AFTER) in supporting this work.

REFERENCES

1 Dieselnet, Emission Standards, 2008, available from http://www.dieselnet.com/standards/.

2 **White, C. M., Steeper, R. R.,** and **Lutz, A. E.** The hydrogen-fueled internal combustion engine: a technical review. *Int. J. Hydrogen Energy*, 2006, **31**(10), 1292–1305.

3 **Jamal, Y.** and **Wyszynski, M. L.** On-board generation of hydrogen-rich gaseous fuels – a review. *Int. J. Hydrogen Energy*, 1994, **19**(7), 557–572.

4 **Docter, A.** and **Lamm, A.** Gasoline fuel cell systems. *J. Power Sources*, 1999, **84**, 194–200.

5 **Dicks, A. L.** Hydrogen generation from natural gas for the fuel cell systems of tomorrow. *J. Power Sources*, 1996, **61**, 113–124.

6 **Naidja, A., Krishna, C. R., Butcher, T.,** and **Mahajan, D.** Cool flame partial oxidation and its role in combustion and reforming of fuels for fuel cell systems. *Prog. Energy Combust. Sci.*, 2003, **29**, 155–191.

7 **Scholte, T. G.** and **Vaags, P. B.** Burning velocities of mixtures of hydrogen, carbon monoxide and methane with air. *Combust. Flame*, 1959, **3**, 511–524.

8 **Rauckis, M. J.** and **McLean, W. J.** The effect of hydrogen addition on ignition delays and flame propagation in spark ignition engines. *Combust. Sci. Technol.*, 1979, **19**, 207–216.

9 **Heywood, J. B.** and **Vilchis, F. R.** Comparison of flame development in a spark-ignition engine fueled with propane and hydrogen. *Combust. Sci. Technol.*, 1984, **38**, 313–324.

10 **Halter, F., Chauveau, C.,** and **Gokalp, I.** Characterization of the effects of hydrogen addition in premixed methane/air flames. *Int. J. Hydrogen Energy*, 2007, **32**(13), 2585–2592.

11 **Milton, B. E.** and **Keck, J. C.** Laminar burning velocity in stoichiometric hydrogen and hydrogen-hydrocarbon gas mixtures. *Combust. Flame*, 1984, **58**, 13–22.

12 **Rafael, S.** and **Sher, E.** Reaction kinetics of hydrogen-enriched methane–air and propane–air flames. *Combust. Flame*, 1989, **78**(3–4), 326–338.

13 **Yu, G., Law, C. K.,** and **Wu, C. K.** Laminar flame speeds of hydrocarbon + air mixtures with hydrogen addition. *Combust. Flame*, 1986, **63**, 339–347.

14 **Coppens, F. H. V., De Ruyck, J.,** and **Konnov, A. A.** Effects of hydrogen enrichment on adiabatic burning velocity and NO formation in methane + air flames. *Exp. Thermal Fluid Sci.*, 2007, **31**(5), 437–444.

15 **Mandilas, C., Ormsby, M. P., Sheppard, C. G. W.,** and **Woolley, R.** Effects of hydrogen addition on laminar and turbulent premixed methane and iso-octane–air flames. *Proc. Combust. Inst.*, 2007, **31**(1), 1443–1450.

16 **Di Sarli, V.** and **Benedetto, A. D.** Laminar burning velocity of hydrogen–methane/air premixed flames. *Int. J. Hydrogen Energy*, 2007, **32**(5), 637–646.

17 **Refael, S.** and **Sher, E.** Autoignition of hydrogen-enriched *n*-butane–air mixture: a theoretical study. In Proceedings of the 23rd International Symposium on *Combustion*, Orleans, France, 22–27 July 1990, 1991, Vol. 1, pp. 1789–1796 (Combustion Institute, Pittsburgh, Pennsylvania).

18 **Li, H., Karim, G. A.,** and **Sohrabi, A.** Knock and combustion characteristics of CH_4, CO, H_2 and their binary mixtures. SAE paper 2003-01-3088, 2003.

19 **Li, H.** and **Karim, G. A.** Knock in spark ignition hydrogen engines. *Int. J. Hydrogen Energy*, 2004, **29**(8), 859–865.

20 **Li, H.** and **Karim, G. A.** Exhaust emissions from an SI engine operating on gaseous fuel mixtures containing hydrogen. *Int. J. Hydrogen Energy*, 2005, **30**(13–14), 1491–1499.

21 **Topinka, J. A., Gerty, M. D., Heywood, J. B.,** and **Keck, J. C.** Knock behavior of a lean-burn, H_2 and CO-enhanced, SI gasoline engine concept. SAE paper 2004-01-0975, 2004.

22 **Nagalingam, B., Duebel, F.,** and **Schmillen, K.** Performance study using natural gas, hydrogen-supplemented natural gas and hydrogen in AVL research engine. *Int. J. Hydrogen Energy*, 1983, **8**(9), 715–720.

23 **Karim, G. A., Wierzba, I.,** and **Al-Alousi, Y.** Methane–hydrogen mixture as fuel. *Int. J. Hydrogen Energy*, 1996, **21**(7), 625–631.

24 **Isherwood, K. D., Linna, J.-R.,** and **Loftus, P. J.** Using on-board fuel reforming by partial oxidation to improve SI engine cold-start performance and emissions. SAE paper 980939, 1998.

25 **Shrestha, S. O. B.** and **Karim, G. A.** Hydrogen as an additive to methane for spark ignition engine applications. *Int. J. Hydrogen Energy*, 1999, **24**, 466–475.

26 **Kirwan, J. E., Quader, A. A.,** and **Grieve, M. J.** Advanced engine management using on-board gasoline partial oxidation reforming for meeting super-ULEV (SULEV) emissions standards. SAE paper 1999-01-2927, 1999.

27 **Smith, J. A.** and **Bartley, G. J. J.** Stoichiometric operation of a gas engine utilizing synthesis gas and EGR for NO_x control. *Trans. ASME, J. Engng Gas Turbines Power*, 2000, **122**, 617–623.

28 **Allenby, S., Chang, W.-C., Megaritis, A.,** and **Wyszyński, M. L.** Hydrogen enrichment: a way to maintain combustion stability in a natural gas fuelled engine with exhaust gas recirculation, the potential of fuel reforming. *Proc. Instn Mech. Engrs, Part D: J. Automobile Engineering*, 2001, **215**, 405–418.

29 **Bauer, C. G.** and **Forest, T. W.** Effect of hydrogen addition on the performance of methane-fueled

vehicles. Part I: effect on S.I. engine performance. *Int. J. Hydrogen Energy*, 2001, **26**(1), 55–70.

30 Bauer, C. G. and **Forest, T. W.** Effect of hydrogen addition on the performance of methane-fueled vehicles. Part II: driving cycle simulations. *Int. J. Hydrogen Energy*, 2001, **26**(1), 71–90.

31 Kirwan, J. E., Quader, A. A., and **Grieve, M. J.** Fast start-up on-board gasoline reformer for near-zero emissions in spark-ignition engines. SAE paper 2002-01-1011, 2002.

32 Tunestål, P., Christensen, M., Einewall, P., Andersson, T., Johansson, B., and **Jönsson, O.** Hydrogen addition for improved lean-burn capability of slow- and fast-burning natural gas combustion chambers. SAE paper 2002-01-2686, 2002.

33 Quader, A. A., Kirwan, J. E., and **Grieve, M. J.** Engine performance and emissions near the dilute limit with hydrogen enrichment using an on-board reforming strategy. SAE paper 2004-01-1356, 2004.

34 Tully, E. J. and **Heywood, J. B.** Lean-burn characteristics of a gasoline engine enriched with hydrogen from a plasmatron fuel reformer. SAE paper 2003-01-0630, 2003.

35 Allgeier, T., Klenk, M., Landenfeld, T., Conte, E., Boulouchos, K., and **Czerwinski, J.** Advanced emission and fuel economy concept using combined injection of gasoline and hydrogen in SI engines. SAE paper 2004-01-1270, 2004.

36 Czerwinski, J. and **Comte, P.** Addition of CNG and reformer gas to the gasoline-fuelled SI engine. SAE paper 2004-01-0973, 2004.

37 Alger, T., Gingrich, J., and **Mangold, B.** The effect of hydrogen enrichment on EGR tolerance in spark-ignited engines. SAE paper 2007-01-0475, 2007.

38 Karim, G. A. Hydrogen as a spark ignition engine fuel. *Int. J. Hydrogen Energy*, 2003, **28**, 569–577.

39 Arrigoni, V., Cornetti, G., Gaetani, B., and **Ghezzi, P.** Quantitative systems for measuring knock. *Proc. Instn Mech. Engrs*, 1972, **186**, 575–583.

40 Heywood, J. B. *Internal combustion engine fundamentals*, 1988 (McGraw-Hill, New York).

APPENDIX

Notations

CAX	timing of X per cent of maximum mass fraction burned on the degrees crank angle basis
COV$_{imep}$	coefficient of variation in the indicated mean effective pressure (per cent)
EGR	exhaust gas recirculation
HC	total of methane and non-methane unburned hydrocarbons
IMEP	indicated mean effective pressure (bar)
MBT	maximum for best torque (spark timing)
MFB	mass fraction burned
NG	natural gas (mostly CH_4 with traces of C_2H_6, N_2, and CO_2)
NO$_x$	nitrogen oxide (NO, NO_2, and N_2O)
RG	reformer gas
SI	spark ignition
TDC	top dead centre
TWC	three-way catalytic converter
λ	ratio of actual air-to-fuel ratio to stoichiometric air-to-fuel ratio
σ_{n-1}	standard deviation of the sampled data corrected for the mean
φ	equivalence ratio $1/\lambda$